International Journal of Advances in Engineering and Management (IJAEM)
Volume 6, Issue 09 Sep. 2024, pp: 626-636 www.ijaem.net ISSN: 2395-5252

Performance Analysis of Solar Water Heaters with Different Tube Configuration Using CFDSimulation (ANSYS FLUENT)

Zayyanu Hussaini *[2], Sadik Umar [1] and Gwani Mohammed[1]
[1] Department of Physics, Kebbi State University of Science and Technology, Aliero
[2] Department of Physics, Federal University of Agriculture, Zuru, Nigeria

Date of Submission: 20-09-2024 Date of Acceptance: 30-09-2024

ABSTRACT
Energy demand is seeing a major increase due to the rise in the standard of living and industrial growth in numerous nations. This has led to the emergence of a substantial gap between energy supply and demand. In this work, design of solar water heaters with different tube arrangement was done and their performance was analyzed using ANSYS FLUENT. The metrological data for Sokoto **(**13° 03' 45.68N, 5° 14' 35.59E) was used to determine the average solar radiation for each month.A numerical study of solar water heaters with different tube configurations has been carried out. The laminar turbulence model was used for flow simulation, whereas the radiation model solver is used to incorporate the radiative element in the energy equation. Two solar water heaters have been designed; performance analysis was numerically investigated. The analysis's findings shows the strong relationship between the outlet temperature and irradiance levels. The maximum outlet temperature recorded for solar water heater with spiral tube arrangement was 68^{O}C and the conventional solar water heater was 60^{o}C at around 12:00 respectively.It also showed that, a solar water heater with a Spiral tube arrangement has the higher efficiency of about 54% compared to 41%at 12:00 hours for the conventional solar water heater. It can be concluded that altering the tube arrangement can improve the performance, therefore, it is very vital to consider the tube configuration in the solar water heater design consider for the performance improvement of solar water heaters.

Key Words. Solar Water heater, ANSYS FLUENT, Spiral, Conventional, Solar Energy, CFD.

I. INTRODUCTION

The world's energy needs are largely met by fossil fuels, which have resulted in significant environmental damage. The combustion of fossil fuels as a source of energy for heating is largely to be blamed for the rise in greenhouse gas levels in the atmosphere. This has resulted in global warming, which has resulted in climate change, floods, forest fires, increasing sea levels, and glacier melting. These are only a few of the negative implications of our excessive reliance on fossil fuels to meet our energy needs. Wind and solar energy, the most plentiful renewable energy sources, are intermittent on a regular and seasonal basis, Kangiwa et al. (2023)

Energy sources can be broadly classified into two categories: renewable and non-renewable. Energy sources that are not able to be replenished quickly are classified as non-renewable, whereas renewable energy sources such as hydropower, solar, wind, biomass, and others can be regenerated naturally. To fulfill its needs, man has, over time, created a variety of technologies and energy sources that can be used for heating. Even though some of these technologies have outdated applications, they are nevertheless in use in some regions of the world.One of the most crucial elements in a nation's social and economic development is its energy supply. A country's economic development can be gauged by its per capita energy consumption, which is also a crucial indicator of global sustainable development. Singal et al. (2007).

Solar water heaters can be used in any weather condition. Houri (2006). The efficacy of these heaters is affected by the amount of solar energy available in the area as well as the temperature of the water entering the system. The overall performance of solar water heating systems has been the subject of several studies. Jaisankar et al. (2011) have published a comprehensive review of solar water heaters. When compared to solar electrical direct conversion systems, which have an

International Journal of Advances in Engineering and Management (IJAEM)
Volume 6, Issue 09 Sep. 2024, pp: 626-636 www.ijaem.net ISSN: 2395-5252

efficiency of only 17%, they found that solar thermal conversion had a 70% efficiency. Solar water heating systems are popular in both the home and industrial sectors because of their ease of use and maintenance.Solar water heaters are classified into two categories: passive and active. The heated water is circulated through the system by a pump in an active solar water heating system. A passive solar water heating system, on the other hand, does not use pumps to transfer the heated water through the system. Because there are no electric components to fail, this form of system is more reliable and easier to maintain than active systems.

Delfn et al. (2000) utilised Matrix Laboratory-based software to simulate a solar home water heating system with variable collector efficiency and variable storage tank volume (MATLAB). Annual simulations for a solar system in Santander, Spain, that includes a solar flat collector, a water storage tank, an auxiliary energy source, and a device for mixing water that produces hot water for a household of four, reveal that systems with a larger volume provide higher solar percentage values. When a larger storage tank was used, however, the solar percentage was less responsive to variations in these parameters.

Marroquín et al. (2013) used the fluid dynamics (CFD) library in the ANSYS simulation program. The CFX-Mesh is used for the mesh, and a face space in the elements between 0.004 and 0.08 m is taken into consideration. The simulation is run under the k-epsilon energy model because of the turbulent flow, and the result varies by 5% from the experiment.

In their study, Eswaran et al. (2014) numerically analysed and carried out a reengineered Ado-Ekide solar water heater using CFD and an experimental study, and the results showed that the CFD result achieved maximum mass flow rate compared to the experimental result. The findings demonstrated that these systems can achieve a maximum mass flow rate of 0.6 kg/s.

Tchuen and Koholé (2018) studied flat plate collector optimisation for solar water heaters using a thermosyphon technique. There is good agreement between the results of the numerical and experimental investigations to create an optimisation system that combines the increased performance of the FPC collector with the ideal parameter design. The results showed that the higher output fluid temperatures and thermal efficiency reached by simulation and experiment were 64.93% and 63.66%, 65.19 and 64.10, respectively.

Islam et al. (2019) numerically analysed a solar water heater using water glycerin and found that water glycerin has maximum efficiency and outlet temperature.

Jiandong et al. (2015) numerically examined an FPC's thermal efficiency and found that the collector's efficiency increased with a decrease in the length or diameter of the collection tube.

Belkassmi et al. (2021) numerically investigated how the employment of copper/water, copper oxide/water, and alumina/water nanofluids affected the functioning of an FPC. The average increases in thermal efficiency with copper/water, copper oxide/water, and alumina/water, respectively, were reported by the authors to be 4.44%, 4.27%, and 4.21%.

Based on the literatures available and consulted the major conclusion drawn is that the performance of solar water heater is influenced by shape of the absorber plate, orientation of the solar water heater, materials used for pipes, and arrangement of pipe etc and there is few data on comparative studies of conventional solar water heater with spiral tube solar water heater using numerical approach.

II. METHODOLOGY

This part encompasses the research design employed in the study, the geographical location where the study took place, the materials utilized, the methodologies employed for data collection, and the methods utilized to evaluate the performance of the solar water heaters.

Materials selection

Material selection is a critical aspect of designing a solar water heater, as the chosen materials can significantly impact the system's efficiency, durability, and overall performance.

ANSYS package 2021 R2
ORIGIN 2022
Microsoft office

Methods

This section begins with the design of geometries using design MODELAR in ANSYS, where all the geometry of the three systems was designed and meshed using ANSYS at the meshing domain. The new project was selected in the ANSYS Workbench by clicking on the "File" menu and choosing "New Project." The analysis type chosen in the Design Modeller was fluid flow, which is the geometry modeling environment within the ANSYS Workbench. The dimensions

International Journal of Advances in Engineering and Management (IJAEM)
Volume 6, Issue 09 Sep. 2024, pp: 626-636 www.ijaem.net ISSN: 2395-5252

and parameters are specified in Table 1. This step involves specifying and assigning geometric parameters, providing geometric restrictions, such as lengths, angles, and distances, that fully specify the models. The geometry quality was then checked to ensure that there were no flaws or inconsistencies.

For the model finite element analysis, an ANSYS Workbench V2021 R2 structural analysis was used for the finite element analysis of the models. Transient state thermal analysis is adopted, while minor modifications in the collector model material use aluminium alloy and copper. The ANSYS workbench is used to design the water heater models.

ANSYS FLUENT software was used to numerically investigate the performance of the solar water heater under identical meteorological conditions. There is a general algorithm for any fluid flow problem in ANSYS FLUENT. This algorithm provides an overview of the steps needed to carry out numerical simulations of real-world flow problems. Nonetheless, the particulars of the flow problem under simulation impact the choices taken at different points in the simulation.

Table 1. Geometrical and Operating Parameters

Dimensions of Tubes	Dimension of shell body (mm)	Length/Quantity (mm)	Material
Storage tank	30	1000	
Pipe	60	2000	Copper
Inlet and outlet diameter	80	30	
Receiver plate	2000x2000	10 thickness	
Evacuated tube	Outer 80 Inner 60	1800	Glass
Fluid domain			Water
Plate			Steel
Mesh		871702	Tetrahedral
Nodes		191418	
Elements		871702	
Iterations		600	

Simulation Setup.

The numerical solutions of the governing equations are obtained using ANSYS. The solar water heater geometry is modelled in the design modular; discretization of the computational domain is also done in the ANSYS meshing package, and the solutions are obtained in the ANSYS Fluent. The solution is obtained from the resulting bundle of ANSYS. The governing equations and boundary conditions are solved using the finite volume methods, which are actualized in the ANSYS Fluent code. A pressure-based solver is used in this study. As part of the ANSYS Fluent Code's solution method, the second-order upwind scheme is used to combine the governing equations with boundary conditions on the computer platform. The pressure-velocity coupling is used for the SIMPLE algorithm. The discrete ordinate model is used to model radiation heat transfer within the receiver tube's annulus space, taking air as a non-participating medium; thus, it is surface-to-surface radiation heat transfer. It is therefore assumed that air does not absorb, emit, or disperse radiation in the evacuated tube. The realizable k.-e is more advanced than the standard realisable k.-e model; it also gives more accurate predictions than the Reynold stress model. The realizable k.-e is more advanced than the standard realizable k.-e model; it also gives more accurate predictions than the Reynold stress model. It is therefore selected for turbulent modelling. The enhanced wall is specifically designed for the near-wall region.

The convergence is monitored by setting the sealed residuals to less than 10^{-4} for continuity, while for momentum, turbulent kinetic energy (k) and turbulence dissipation rate (e) are less than 10^{-5}, and energy residuals are set to be less than 10^{-7}. The solution is run more than 150 successive iterations until the scaled residual has ceased to change. At this point, the solution converged.

Crafting and scrutinizing a solar water heater in ANSYS Fluent involves several steps, such as fabricating the geometry, configuring the simulation, delineating the boundary conditions, and dissecting the outcomes. General set-up, transient was selected, and pressure-based absolute

International Journal of Advances in Engineering and Management (IJAEM)
Volume 6, Issue 09 Sep. 2024, pp: 626-636 www.ijaem.net ISSN: 2395-5252

velocity formulation was also selected. The energy equation was activated, and the flow was selected as laminar. For pressure, momentum, and energy, a second-order upwind equation was also selected. To get an acceptable result, the residual factor was set to.

The Pre-processing Stage

This is the initial stage of the ANSYS FLUENT simulation process, which aids in providing the most accurate geometry description. These are some of its smaller steps:

- ✓ Geometry
- ✓ Physics model
- ✓ Material properties
- ✓ Boundary conditions
- ✓ Initialization

Geometry

Geometry is a very important parameter in designing a model in ANSYS software. At this part, the solar water heater system was created in the modular design domain by selecting the appropriate shape/figure to extrude using the given dimensions. The designed models are shown in Figure 1 which include the solar collector, pipes, and storage tank.

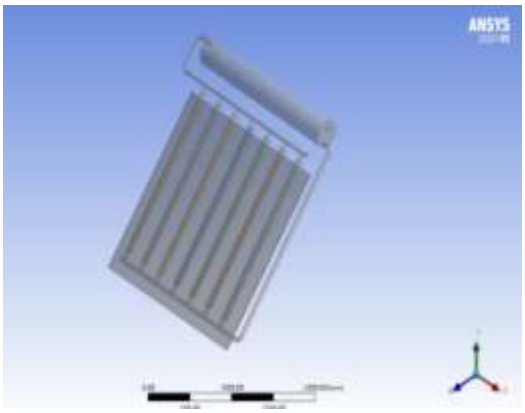

Figure 1 Geometry Part Of The conventional Solar Water Heater

Meshing Generations

The process of meshing in ANSYS Fluent comprises multiple processes aimed at creating a mesh of superior quality that precisely captures the geometry and physics of the simulated situation. The process was initiated by directly constructing geometry within ANSYS Design Modeller and importing it to the meshing part. The parameters were set by specifying the meshing type, element sizes, inflation layers, and other meshing variables. Meshing was generated using a specified setting. Due to the need for high-dependability outcomes, it was important to create an efficient mesh with an appropriate number of nodes and elements, as indicated in Figures 2 and Figure 3. However, a comparative analysis was performed between a variety of meshes with different qualities and numbers of elements, as shown in Table1, to verify the efficiency of the mesh in this work. As a result, tetrahedral was employed because it was well-suited for some scenarios, such as its flexibility, adaptability, accuracy in capturing flow features, and modeling of physics.

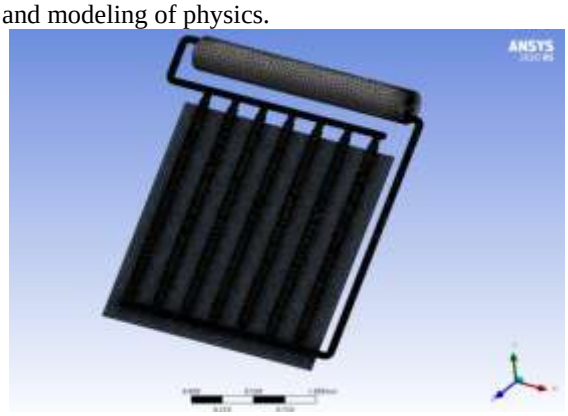

Figure 2 Meshing part of conventional tube SWH

The solar water design in Figure 2 and Figure 3 was created with Ansys Fluent and was ready for the CFD simulation process. All of the geometry was created for the CFD simulation preparations. The CFD solver uses the computational mesh as a pre-processor.

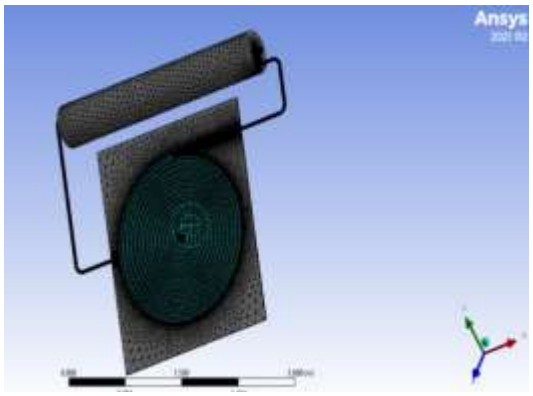

Figure 3 Meshing part of the SWH with Spiral tube Arrangement

ANSYS FLUENT software is used to mesh and fix the geometrical errors in all three solar water heater models. Boundary conditions are then applied and the solution is initialised. The meshed model of the solar water heaters (conventional and Spiral tube arrangements) is displayed in Figure 2 and Figure 3.

International Journal of Advances in Engineering and Management (IJAEM)
Volume 6, Issue 09 Sep. 2024, pp: 626-636 www.ijaem.net ISSN: 2395-5252

Boundary Conditions Setup

Water was selected as the working fluid, and the wall material is copper. A transient analysis is performed. The 300K was selected as the outside temperature. The following boundary conditions apply to both absorber tubes. The water's inlet temperature is 300 K. The velocity of the water flowing within the absorber tube is varied from 0.1 to 2.0m/s, at each point, the water's outlet temperature is almost equal to the inlet temperature. The fluid flowing inside the absorber tube is given the inlet boundary conditions. The water is given inlet boundary conditions (Temperature and Velocity). The working condition are giving in the Table 1. It was determined that the inlet's mass flow rate was 0.008 kg/s.The outlet is equipped with a boundary condition that ensures the continuity equation is satisfied. The thermal efficiency of the solar water heaters was determined by simulation from 7:00am to 17:00 hours. To achieve this, the following assumptions were made.

- Liquid Material - Water
- Energy condition -ON
- Turbulence Model - laminar
- Solution Method Second Order.
- Material – copper and steel
- The rear surface of the collectors is fully insulated

The parameters are applied to all the three designs.

Solver

As a transient-state conjugate heat transfer problem, the computational domain has been addressed, and the process of solution is carried out up until convergence and an accurate mass and energy balance are attained. The iterative approach involves solving each problem repeatedly for a predetermined amount of time until the convergence requirements are satisfied. The heat balance equation (Energy-on) is used to calculate the heat transfer between the light-absorbing surface and the air. The solar calculator in ANSYS is used to compute the quantity of solar radiation, which allows the intensity of solar radiation to be determined. A second-order upwind approach is used to solve the system of differential equations representing heat and mass transport processes. A convergence criterion of was set based on concerns about minimising computing calculations. There have been 600 iterations, as stated in Table 1. The convergence of the solution in varied situations occurs between 350 and 500 iterations. However, after the physics problem has been recognised, the following procedures are used to address it using a computer: fluid material attributes, flow physics model, and boundary conditions.

Initialization

Based on the free surface level of the chosen zone from the Compute from list, the volume fraction will be patched in the domain. The constant value given for the velocity magnitude in the chosen zone will be used to patch the velocities within the domain. Two different kinds of initialization methods exist. Standard initialization and hybrid initialization. In this research, the standard initialization is used. The fluid (water) is employed as a reference frame and the values are computed from the inlet temperature.

Post Processing

After receiving the results, the next step is to analyse them using various techniques, such as contour plots, streamlines, vector plots, etc.

Solution Processor

In the current simulation, momentum, energy, and the governing equations of continuity are solved using ANSYS FLUENT's finite volume approach in the transient domain. It is decided to use a second-order upwind strategy for both the energy and momentum equations. Double precession was selected. All of the transport equations used the second-order upwind discretization approach. The solution begins using the first-order upwind discretization scheme and continues using the second-order upwind method whenever convergence issues are identified. In a transient state, the governing equations for mass and momentum conservation are solved sequentially using implicit linearization.

Determination of design month.

From the observations in Table 2, August and September have the lowest value of irradiance yearly. Better performance during other months of the year would be made possible by using irradiance values from these two months in the system design. As a result, the month of August is chosen as the design month.

International Journal of Advances in Engineering and Management (IJAEM)
Volume 6, Issue 09 Sep. 2024, pp: 626-636 www.ijaem.net ISSN: 2395-5252

Table 2 monthly Solar irradiance of Sokoto

Month	Global Horizontal Irradiance (GHI) (kWh/m^2 /day)
January	5.7
February	6.3
March	6.6
April	6.5
May	6.1
June	5.7
July	5.4
August	5.1
September	5.2
October	5.7
November	5.7
December	5.5

The computation of system design parameters and subsequent component sizing was done based on the design month's average daily solar radiation and meteorological data of Sokoto since the demand on the system during the design month is typically the highest. To establish the design month, the weather data processor's monthly average daily weather data and solar radiations on the collector's surface for all months were used. To determine the energy ratio, E_R programming codes were generated using the ANSYS software as input.
Collector Sizing Based on Required Heat Energy

The solar collector is sized based on how much thermal energy the system needs. In determining the collector area, other factors to consider are the irradiance values at the system location and the collector efficiency. The collector effectiveness can be determined by using equation 1

$$\eta = \frac{\dot{m} c_p \Delta T}{I A_c} \qquad 1$$

where I is solar irradiation, η represents collector efficiency, ṁ represents mass flow rate, A_c represents collector area, T is the temperature change and it is measured in square meters m^2.
Efficiency is typically less than 100% because there are inefficiencies such as friction and heat loss that convert the energy into alternative forms. Equation 3.1 was used to determine the efficiencies of the systems. Gargee, et al (2015).
To determine the collector area, equation2 can be written as

$$Ac = \frac{Qu}{\eta I} \qquad 2$$

Rikoto & Garba, (2015) stated that collector efficiency ranges from 0.4 to 0.6, and since the system design assumes an efficiency of 58% with I = 4.5 kWh/m^2/day, the. collector area necessary to generate the thermal energy of 2 kWh was calculated to be 0.75 m^2.

Performance Analysis

Performance analysis is critical for determining if a system is fulfilling its function well and whether it is profitable. It enables specialists to understand which technology performs better, which heat transfer fluid is more efficient, and what the system's limitations are.
The temperatures inlet and outlet with mass flow rate were measured and Equation 3 was used to compute the performance

$$Q_u = mc_p(T_{f_0} - T_{f_i}) \qquad 3$$

Where, Q_u is the rate of useful energy gained, m is the mass flow rate of fluid flow, C_p is the heat capacity of water or working fluid and T_{f_0} and T_{f_i} are the inlet and outlet fluid temperature of the solar collector. The useful energy can also be expressed in terms of the energy absorbed by the absorber and the energy lost from the absorber as given by

$$Q_u = A_C F_R[I(\tau\alpha) - U_L(Tf_i - T_a)] \qquad 4$$

Where F_R is the 'collector heat removal factor' defined as the ratio of the actual heat transfer to the maximum possible rate, A_C is the surface area of the solar collector, I is the global solar radiation, is the absorptance–transmittance product, U_L is the overall loss coefficient of solar collector, and T_a is the ambient temperature.

$$Q_u = A_C F_R[I(\tau\alpha) - U_L(Tf_i - T_a)] \qquad 5$$

International Journal of Advances in Engineering and Management (IJAEM)
Volume 6, Issue 09 Sep. 2024, pp: 626-636 www.ijaem.net ISSN: 2395-5252

The relation between the collector efficiency factor and the heat removal factor F_R will be determine using equation 7

$$F_R = \frac{mc_p}{A_C U_L}\left[1 - \exp\left(-A_C U_L F/mC_p\right)\right] \qquad 6$$

The instantaneous collector efficiency relates the useful energy to the total radiation incident on the collector surface by equation 7

$$\eta = \frac{T_{out} - T_{in}}{T_{out}} \text{ x } 100 \qquad 7$$

T_{out} Is the temperature of the hot water exiting the solar collector? T_{in} is the temperature of the cold water entering the collector.

System Design Approach

A solar water heating system's component must be appropriately sized for satisfactory performance and dependability, as well as accurately predicted system performance (such as provided useable energy and output water temperature, solar percentage, and thermal efficiency, among other factors). To achieve adequate performance, it is crucial to size system components appropriately and determine system characteristics by computing system design parameters. The above design process was used to determine these design parameters and assess their sensitivity and impact of specific design factors on the functionality of the solar water heating system.

Data Processing and Analysis

Temperatures at the inlet and outlet, solar radiation, collector size, and storage tank capacity, were measured and observed using standard measuring tools that have been validated and are pertinent to the variables under investigation. The Origin software was utilized to process the gathered data. The data presented herein includes tables and graphs, such as line and bar graphs. The impact of storage tank capacity, collector size, collector orientation, and inlet and outlet temperatures were examined, and conclusions regarding the operation of solar water heaters were drawn in light of the research findings.

The data in this study was analyzed using ANSYS software, which was then used to calculate the analysis of a solar water heating system and calculate the savings obtained through the use of SWH. A dynamic software tool called ANSYS is used to simulate and optimize solar thermal systems, including space heating and hot water systems. Three different tube arrangements—Spiral and conventional—are the foundation for the ANSYS approach used in this research to simulate and analyze the performance of the solar water heating system.

III. RESULT AND DISCUSSIONS

This chapter presents a comprehensive summary of the outcomes obtained from simulations conducted for the two solar water heater models that were designed. The system's numerical accuracy was verified by ensuring the fulfillment of the continuity equation. The ambient Temperatures fitted with solar water heaters were recorded at one-hour intervals between 7.00 hours and 17:00 hours, and the inlet, outlet, and ambient temperatures with solar irradiance were observed and recorded. The figures were extracted from ANSYS FLUENT results.

The analytical findings include a calculation of the energy produced by the solar water heater and needed for the systems. The results of the simulation are shown in Figure 4.2 to Figure 4.13, which also shows the direction of water flow between the outlet and inlet at different mass flow rates as well as values for temperature contour, pressure contour, velocity stream, velocity contour, velocity vector, and volume rendering profile of the collectors. After providing the software with all the necessary data, such as the properties of the different tube arrangements shown in the tables and figures, it carried out the calculations and outputted the results in the form of graphs, reports, and contours for the parameter distribution.

The quantity of energy received in locations differs, due to factors such as latitude, altitude, atmospheric conditions, and more. To gather data on radiation levels it is necessary to determine the latitude and longitude of a place. This enables us to calculate the amount of sunlight received from the sun yearly at different angles and slopes, for the desired location. In this study, Sokoto, Sokoto State, Nigeria is a case study.

The temperature contour, pressure contour, and airflow velocity at all node sites in the model duct were all measured using ANSYS FLUENT 2021 R2.

International Journal of Advances in Engineering and Management (IJAEM)
Volume 6, Issue 09 Sep. 2024, pp: 626-636 www.ijaem.net ISSN: 2395-5252

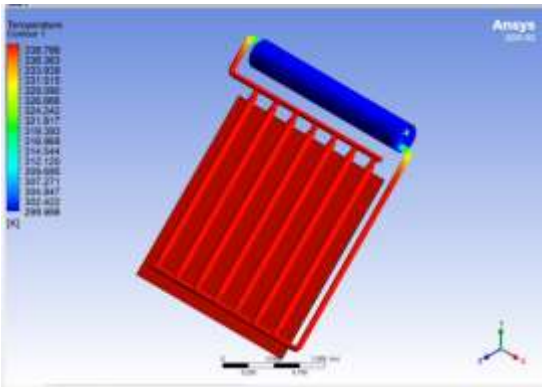

Figure 5 Temperature profile obtained from the straight tube SWH

Figure 5 describes the temperature contour of a solar water heater with a straight tube arrangement. The Figure also illustrates how the output contour temperature of the fluid domain portions was displayed in colour, with a temperature of 338.7K. The displayed value varied based on changes in the locations of the places where the temperature contour varied. In the legend, blue color represent the least temperature while the red color indicat the maximum temperature.

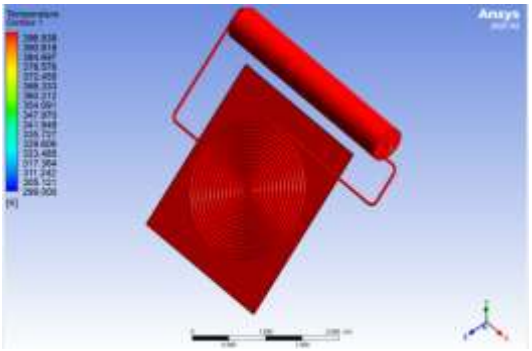

Figure 6 Temperature profile obtained from the spiral tube SWH

The temperature contour of the solar water heater with spiral tube arrangement is shown in Figure 6, with the inlet coming from the far-left end of the model and the heat source coming from the top. The Figure also shows the temperature contour of a solar water heater, with the heat source coming from above and the inlet coming from the far end of the model. In the legend on the left side of the model, blue represent the least value and red represent the maximum value. The higher temperature, 338.788 K and for conventional and 396.939k for spiral.

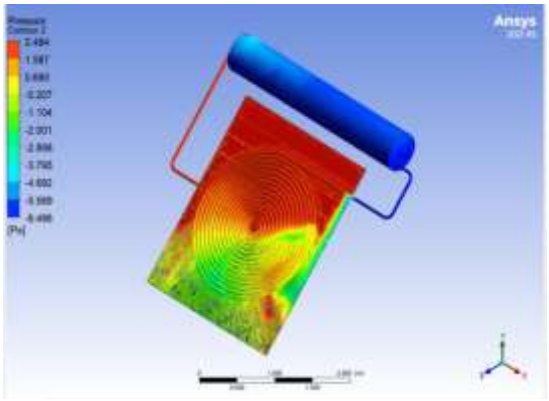

Figure 7. Pressure contour of spiral tube

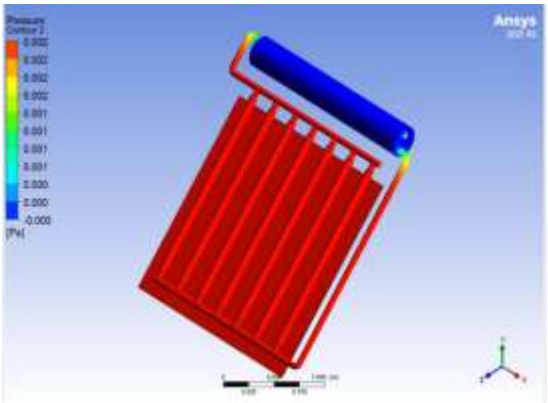

Figure 8 Pressure Contour of Straight Tube SWH

Figure 8 shows the pressure profile, with a steady reduction in pressure in the direction of the outlet. Figure 8 and Figure 9 demonstrates the velocity profile for different mass flow rates.

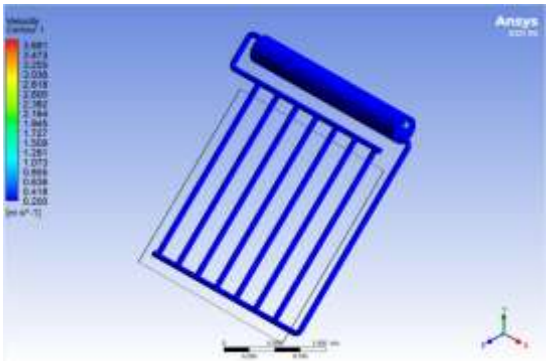

Figure 9 Velocity Contour of Straight Tube SWH

Figure 9 shows the velocity contour of solar water heater with straight tube arrangements as the upper side wall, or absorber plate, receives insolation (heat flux), the temperature there is quite high, and due to insolation, it drops in the direction of the lower wall. It is obvious that the static temperature (heat flux) of the flow field drops as

International Journal of Advances in Engineering and Management (IJAEM)
Volume 6, Issue 09 Sep. 2024, pp: 626-636 www.ijaem.net ISSN: 2395-5252

the mass flow rate rises. The diffusion of temperature into the flow field's core increases as the mass flow rate rises, but the diffusion of temperature near the wall decreases as the mass flow rate rises.

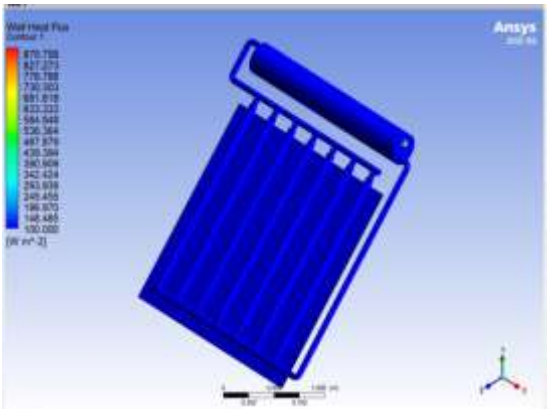

Figure 10 Heat Flux Contour For Straight Tube SWH

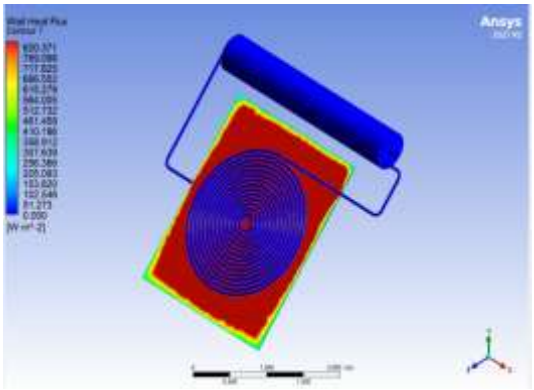

Figure 1 Heat Flux Contour for Spiral Tube SWH

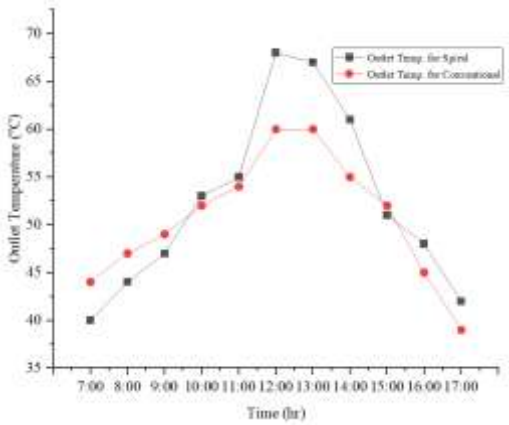

Figure 12. Graph Of Outlet Temperatures Against Time

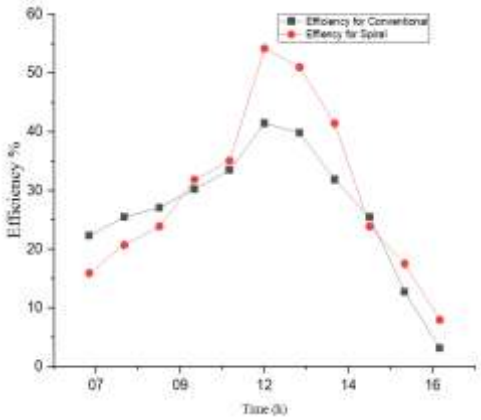

Figure 13. A graph of Efficiency against Time

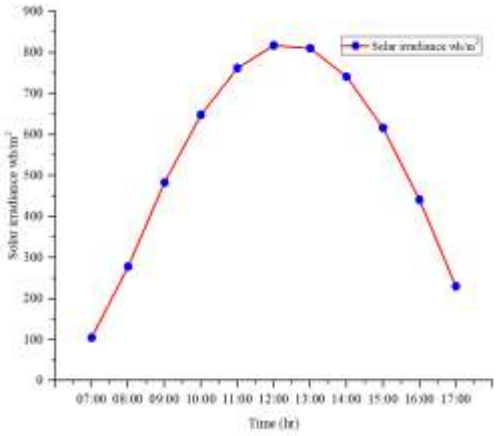

Figure 14 Variation of solar Irradiance with respect to Time

From the Figure 12, it is seen that outlet temperature raises slowly during the first few hours, but then increases until its peak at 12:00 hours It is worth noting that the irradiance levels peak an hour before the outlet temperature. The highest outlet temperature attained is solar water heater with spiral tube arrangement with 68^{0}C at about 12:00 hours while conventional solar water heater recorded 60^{0}C at the same time. It can be noted that there is a close relationship between conventional solar water heater and solar water heater with Spiral arrangement. From the graph, it is evident that the tubes arrangements have a significant impact on temperature of solar water heaters.

Figure 14 shows the solar irradiance gradually rises from 7:00 hours to 12:00 hours, peaking at 917 W/m^2 at around 13:00 hours and it will start declining at around 14:00 hours till it reaches 230 W/m^2 at 17:00 hours.

International Journal of Advances in Engineering and Management (IJAEM)
Volume 6, Issue 09 Sep. 2024, pp: 626-636 www.ijaem.net ISSN: 2395-5252

Figure 12, however, shows that temperature rise varies according to the time of day. As time passes, the insolation increases, as does the temperature, with the highest values observed at 13:00 hours in all tube arrangements, and then the temperature begins to decline from 15.00 hours to 16.00 hours.

IV. CONCLUSION

The current study uses the ANSYS software to design and simulate a water heating system, replicating the climatic conditions of Sokoto. Several simulations were run at various times, which had an impact on the working fluid's ability to transfer thermal energy and produce a range of results.

ANSYS Fluent was used to simulate the solar water heater in order to compare and forecast the system performance, guarantee system efficiency, and make all required adjustments to achieve the highest possible system performance.

From the result above, it is clear that conventional solar water heater recorded the lowest outlet temperature, 60^0 C while solar water heater with Spiral tube arrangement recorded 68^0C at 12:00 hours

Based on the research's findings, it can be concluded that a solar water heater with a Spiral tube arrangement has a higher efficiency of about 54% compared to 41% at 12:00 hours for the conventional solar water heater. It can be concluded that the tube arrangement is very vital in the performance of solar water heaters.

REFERENCE

[1]. Belkassmi, K., Gueraoui, L., elmaimouni, N., Hassanain, and Tata, O. (2021) "Numerical investigation and optimization of a flat plate solar collector operating with $Cu/CuO/Al_2O_3$–Water nanofluids," Transactions of Tianjin University, vol. 27, no. 1, pp. 64–76.

[2]. Dao Danh Tung and Shuichi Torii (2011). "Heat transfer performance of a self-oscillating heat pipe using pure water and effect of inclination to this performance". Department of Mechanical System Engineering, Kumamoto University, 2-39-1 Kurokami, Kumamoto 860-8555, Japan

[3]. Delfín, S. S., Carlos R. E., and Valentín,C .H. (2000). "Simulation of a solar domestic water heating system, with different collector efficiencies and different volume storage tanks". http://sel.me.wisc.edu.

[4]. Eswaran, E., Chanduru, M., Vairavel, M., and Girimurugan, R. (2014) "Numerical Study on Solar Water Heater Using CFD Analysis "International Journal of Engineering Sciences and Research Technology. 3 (3) pp 1485-1489

[5]. Houri, A., (2006) "Solar water heating systems in Lebanon: current status and future prospects". Renewable Energy: An Inter. J., 31, 663-657

[6]. Islam,T., Zaman,M.S.B., Rashid, F. and Hoque, M.E. (2019) "Numerical analysis of Solar Water Heater Using Water-Glycerine solution" International Conference on Mechanical, Industrial and Materials Engineering. pp 17-19. paper ID ET-18

[7]. Jaisankar, S., Ananth, J., Thulasi, S., Jayasuthakar, S.T. and Sheeba, K.N., (2011). "A comprehensive review on solar water heaters". Renewable & Sustainable Energy Reviews, 15, 3045-3050

[8]. Jiandong, z., Hanzhong, T., and Susu, C. (2015) "Numerical simulation for structural parameters of flat-plate solar collector," Solar Energy, vol. 117, pp. 192–202, 2015

[9]. Kangiwa, U. M., Mohammed, G., Hussaini, Z. and Umar, S. (2023). "Numerical Design of an Off-Grid Wind Energy Systems for Small Scale Residential Power Supply". Journal of Energy Research and Reviews, 15(1), 47–57. https://doi.org/10.9734/jenrr/2023/v15i1297

[10]. Koholé Y., W. and Tchuen, G. (2018) "Experimental and numerical investigation of a thermosyphon solar water heater," International Journal of Ambient Energy, vol. 0750, no. May, pp. 1–11.

[11]. Karthick, K. K. Murugavel, and P. Ramanan, (2018) "Performance enhancement of a building-integrated photovoltaic module using phase change material," Energy, vol. 142, pp. 803–812.

[12]. Kazuz M.R. (2014). "Hybrid solar thermos-electric systems for combined heat and power" PhD thesis .pdf. Cardiff University.

[13]. Kishor, N., Das, M.K., Narain, A., and Ranjan, V.P. (2010) "Fuzzy model representation of thermosyphon solar water heating system", Solar Energy, 84 (6) 948-955.

[14]. Manoj, P. K., K. Mylsamy, and P. T. (2020) "Saravanakumar, "Experimental investigations on thermal properties of nanoSiO2/paraffin phase change material (PCM) for solar thermal energy storage applications," Energy Sources, Part A: Recovery, Utilization, and Environmental Effects, vol. 42, no. 19, pp. 2420–2433.

[15]. Moravej, M., Saffarian, M. R., Li, K. B., Doranehgard, M. H., and Xiong, Q. (2020) "Experimental investigation of circular flat panel collector performance with spiral pipes," Journal of Thermal Analysis and Calorimetry, vol. 140, no. 3, pp. 1229– 1236.

[16]. Marroquin-De, D. J., Olivares-Ramirez, J. M., Omar, J. S., Antonito, Z. A. And Armando, E. O. (2013) "Analysis of flow and heat transfer in a flat solar collector with rectangular and cylindrical geometry using CFD," Ingeniería, Investigación y Tecnología, vol. 14, no. 4, pp. 553–561.

[17]. Rikoto, I. I., & Garba, M. M. (2015). "Design, Construction and Installation of 250-Liter Capacity Solar Water Heating System at Danjawa" Renewable Energy Model Village. 4, 39–44.

[18]. Samson, A.A. (2013) Performance of Solar Water Heater in Akure, Nigeria. Journal of Energy Technologies and Policy, 3(6), 1-8.